Supporting Information

Novel 2D Silica Monolayers with Tetrahedral and Octahedral Configurations

Gaoxue Wang[1], G. C. Loh[1,2], Ravindra Pandey[1*], and Shashi P. Karna[3]

[1]Department of Physics, Michigan Technological University, Houghton, Michigan 49931, USA
[2]Institute of High Performance Computing, 1 Fusionopolis Way, #16-16 Connexis, Singapore 138632
[3]US Army Research Laboratory, Weapons and Materials Research Directorate, ATTN: RDRL-WM, Aberdeen Proving Ground, MD 21005-5069, U.S.A.

---

1. Structure search by the particle swarm optimization (PSO) method (CALYPSO program package)

The structural search was performed by using the particle swarm optimization (PSO) method as implemented in CALYPSO code [1-4]. PSO is a method for multidimensional optimization, which is inspired by the social behavior of birds flocking [2]. It can predict the crystal structure with the known chemical composition at given external conditions, which has successfully utilized for the structure prediction of lithium-boron compounds at high pressure [5] and other 2D materials [6]. In our case, the structures with the SiO_2 stoichiometry are considered for calculations. The number of structures (e.g., population) that produced at each step is set to 24, and the number of CALYPSO steps (e.g., generation) is fixed to 30. The required structural relaxation by CALYPSO was performed using the Perdew-Burke-Ernzerhof (PBE) [7] exchange correlation functional to density functional theory (DFT) [3].

Figures S1, S2, and S3 show the history of structural search by CALYPSO. For the unit cell with 3 atoms, only *O*-, and *T*-silica are predicted as the energetically preferred monolayer as shown in Figure S1.

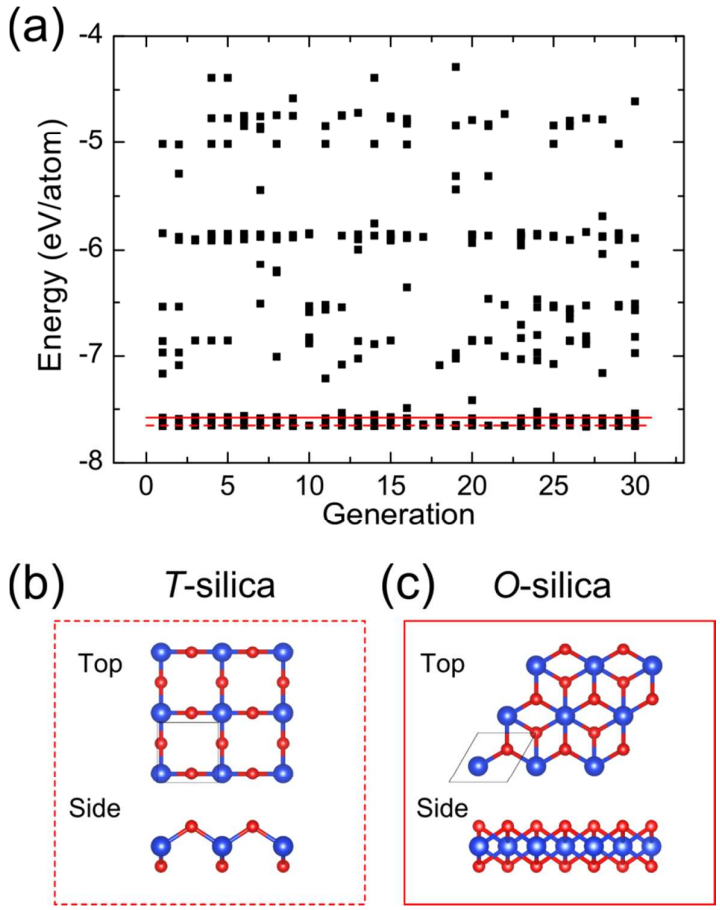

Figure S1. (a) The history of structural search by CALYPSO for the unit cell with 3 atoms *(Si:O=1:2). O-, and T-silica are predicted as the energetically preferable structures as illustrated by the red lines. (b) and (c) are the structural configurations of T- an O-silica, respectively.*

For the unit cell with 6 atoms, other stable structures are also obtained besides *T*- and *O*-silica. *T'*-silica can be obtained by flipping 1/2 of the SiO_4 tetrahedrons in *T*-silica, though its 'top' view is similar to that of T-silica. *T'*-silica has a distorted surface compared to *T*-silica, it will not therefore be further discussed in this paper. Other possible structure as shown in Figure S2(c) will not be considered for further calculations due to its structural complexity.

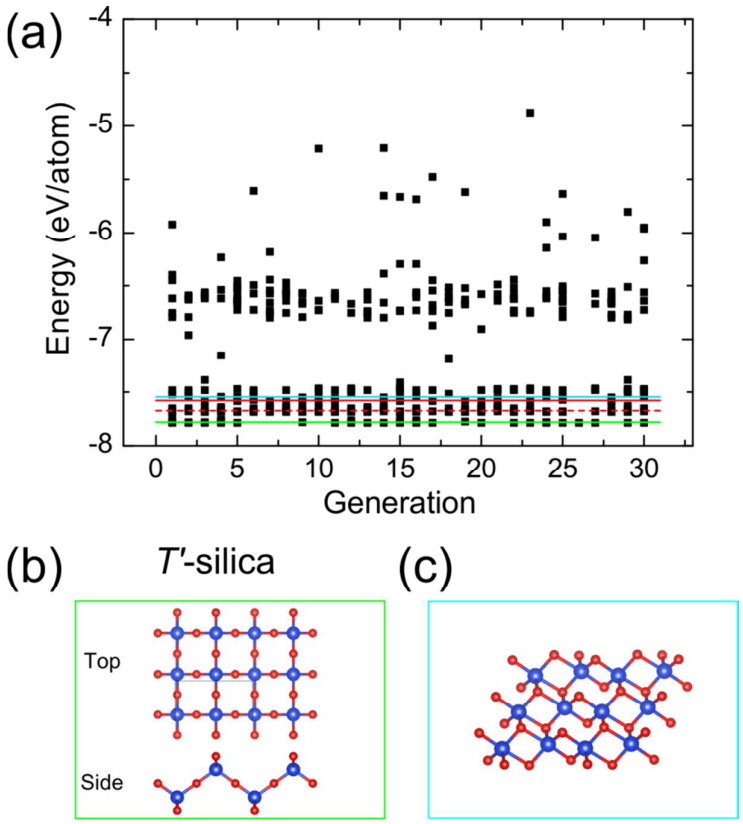

Figure S2. (a) The history of structural search by CALYPSO for the unit cell with 6 atoms *(Si:O=2:4). Red lines show T-, and O-silica, and other possible structuers are shown in (b) and (c).*

For the unit cell with 9 atoms, *O*-, *T*- and *T'*-silica are obtained together with the other structures with tetrahedral building blocks as shown in Figures S3(b) and S3(c).

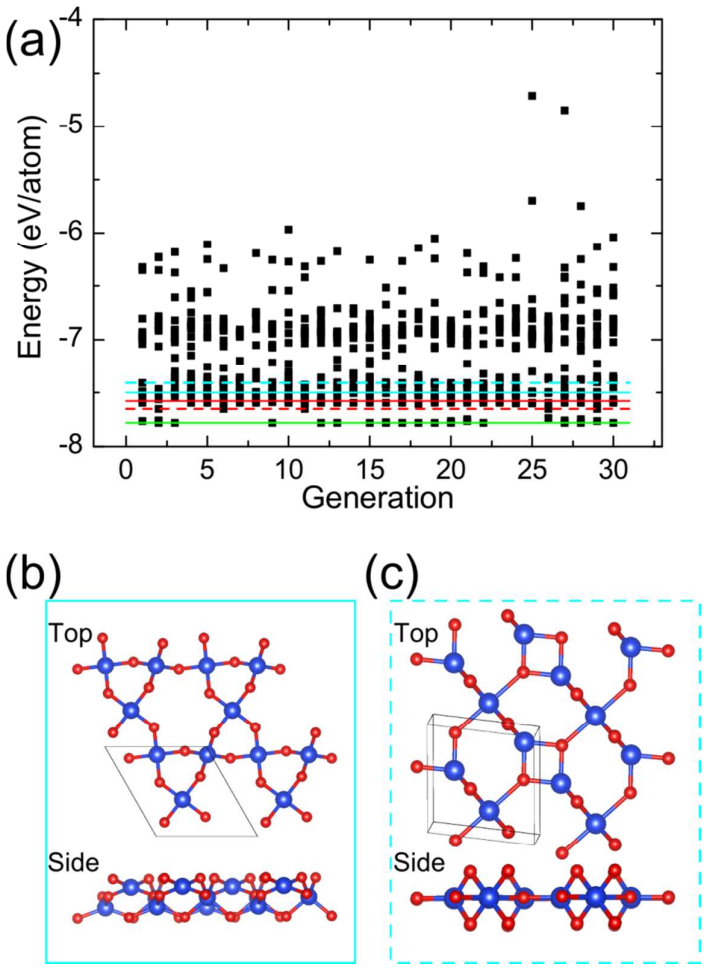

Figure S3. (a) The history of structural search by CALYPSO for the unit cell with 9 atoms *(Si:O=3:6). Red lines show T-, and O-silica, and green lines show T'-silica, other possible structuers are shown in (b) and (c).*

2. Structural and electronic properties of α-silica

In α-silica, each Si is threefold-coordinated either by coplanar O atoms (forming sp^2 bonds) or non-coplanar O atoms (forming sp^3 bonds). The sp^3 bonded Si atom occupies one corner of the tetrahedron, three O atoms occupy the other three corners, as seen from Figure S4(a). $R_{Si\text{-}O}$ of the sp^3 bonds is 1.83 Å, and $R_{Si\text{-}O}$ of sp^2 bonds is 1.62 Å. It is a semiconductor with the VBM contributed by sp^3 bonds, and CBM contributed by sp^2 bonds as seen in Figure 4(c).

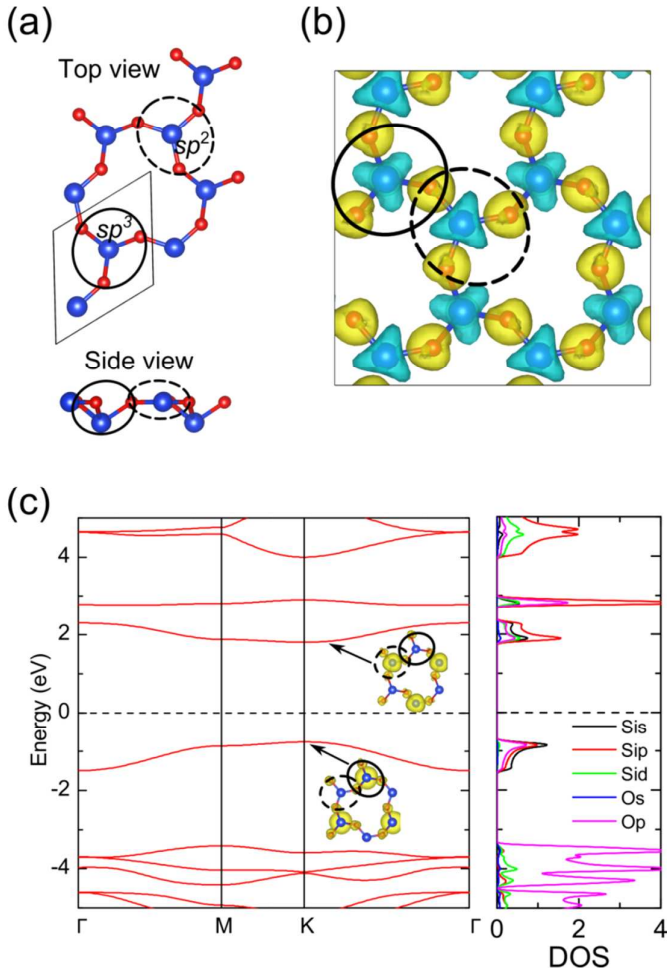

Figure S4. α-silica. (a) Atomic structure where solid (dashed) circle illustrates the sp^3 (sp^2) bonds, (b) deformation electron density (with isosurface of 0.01 e/Å^3). Blue represents depletion of electrons, and yellow represents accumulation of electrons, (c) electronic band structure and DOS, inset shows the charge density at VBM and CBM.

3. Formation energy of α-silica and silicatene

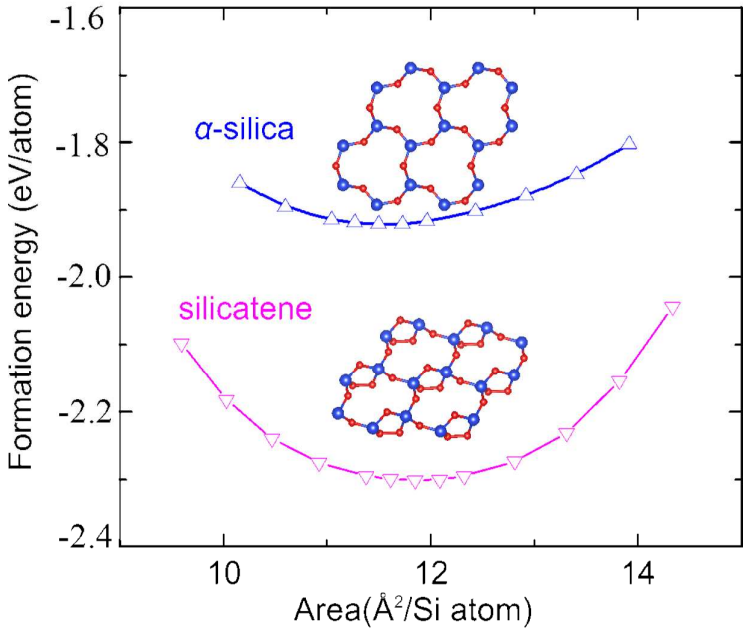

Figure S5. Formation energy of α-silica and silicatene.

4. QTAIM analysis

The Si-O bond nature in the 2D silica allotropes is investigated by analyzing the topology of electron density with the quantum theory of atoms in molecule (QTAIM)[8-9]. The calculations were performed with the Perdew-Burke-Ernzerhof (PBE) functional form and the plane-wave basis sets as implemented in VASP.

Figure S6 shows the electron localization function (ELF) for 2D silica configurations. A large *ELF* around O atoms is mainly due to the difference of electronegativity between Si and O atoms. Tetrahedral configurations of silica bilayer

and *T*-silica lead to similar ELF around the oxygen atom whereas the *ELF* of *O*-silica shows triangular shape reflecting the threefold-coordinated nature of O atoms.

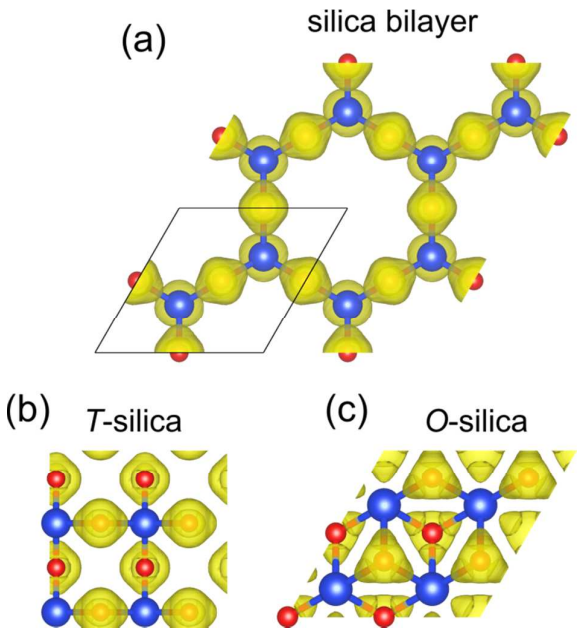

Figure S6. Electron localization function (ELF) for bilayer silica, T- and O-silica with the isosurface at the isovalue of 0.8.

\

The charge density and Laplacian plots (Figures S7(a) and S7(b)) also similarity in the nature of the Si-O bonds in silica bilayer and *T*-silica. In contrast, the Si-O bond in *O*-silica has more ionic characteristics as shown by the separated zero envelope of the 2D Laplacian (Figure S7(b)).

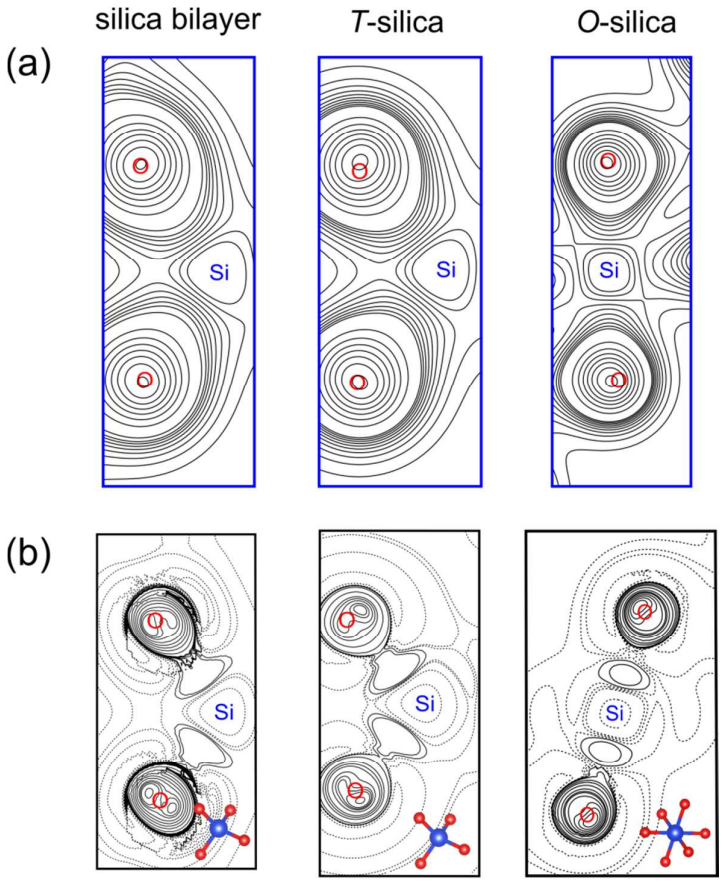

Figure S7. 2D charge density contours (a) and Laplacian (b) for silica bilayer, T- and O-silica.

5. STM images

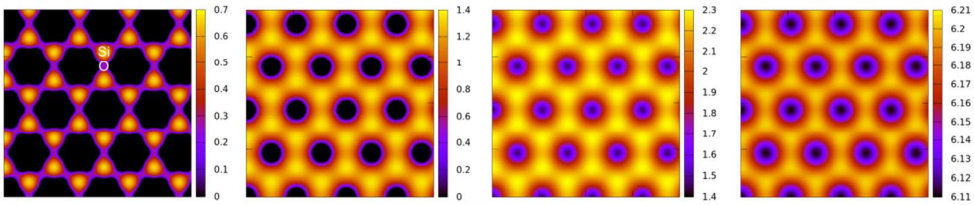

Figure S8. STM images of freestanding silica bilayer under bias voltages of 2.5 V, 2.55 V, 3 V, and 4 V.

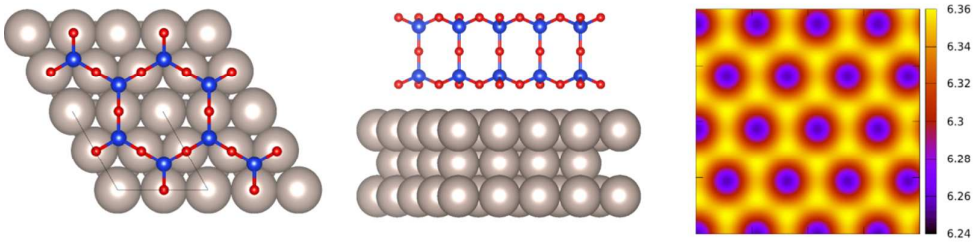

Figure S9. Structure and STM images of bilayer silica on Ru(0001) surface.

6. T- and O-silica nanoribbons

For *T*-silica, we only considered the configuration by cutting along the line in which the edge is terminated by alternating Si and O atoms as illustrated by the shadowed region of Figure S10(a). For *O*-silica, cutting along the zigzag direction leads to edges terminated by Si (Si edge) or O atoms (O edge). Therefore, there exists three kinds of zigzag nanoribbons; (i) both edges terminated by O (O-O zigzag), (ii) both edges terminated by Si atoms (Si-Si zigzag), and (iii) one edge terminated by O and the other terminated by Si atoms (Si-O zigzag). On the other hand, cutting along the armchair direction yields the armchair nanoribbons with symmetric edges, or asymmetric edges (Figure S10 (b)).

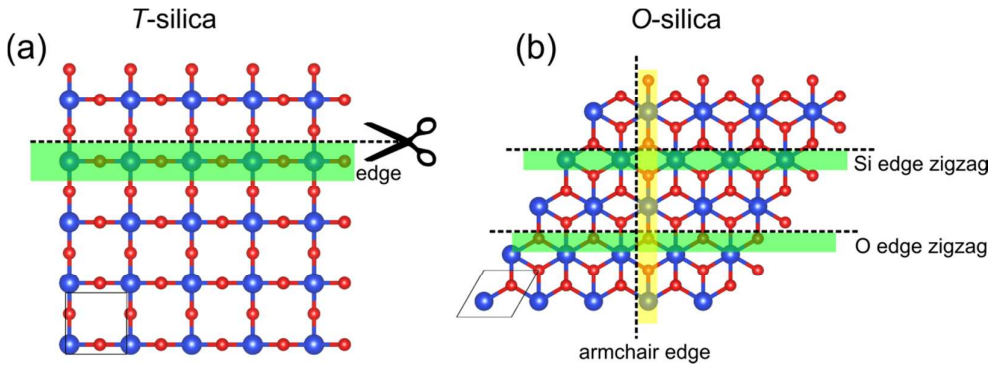

Figure S10. T- and O-silica nanoribbons. The dashed line shows the cutting position, and the hadowed region shows the atoms at the edge of the nanoribbons.

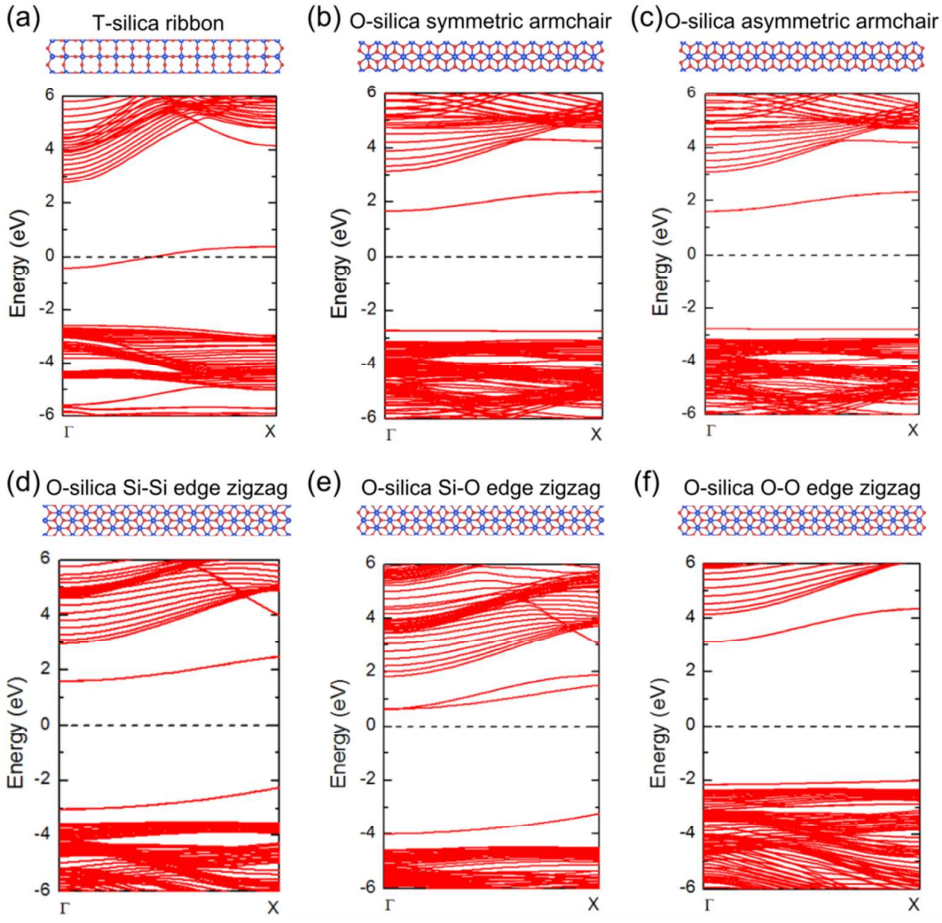

Figure S11 Nanoribbons – Structure and band structure of T-silica and O-silica nanoribbons. The widths of nanoribbons are about 40 Å.

7. Band structure of Graphene/O-silica bilayer

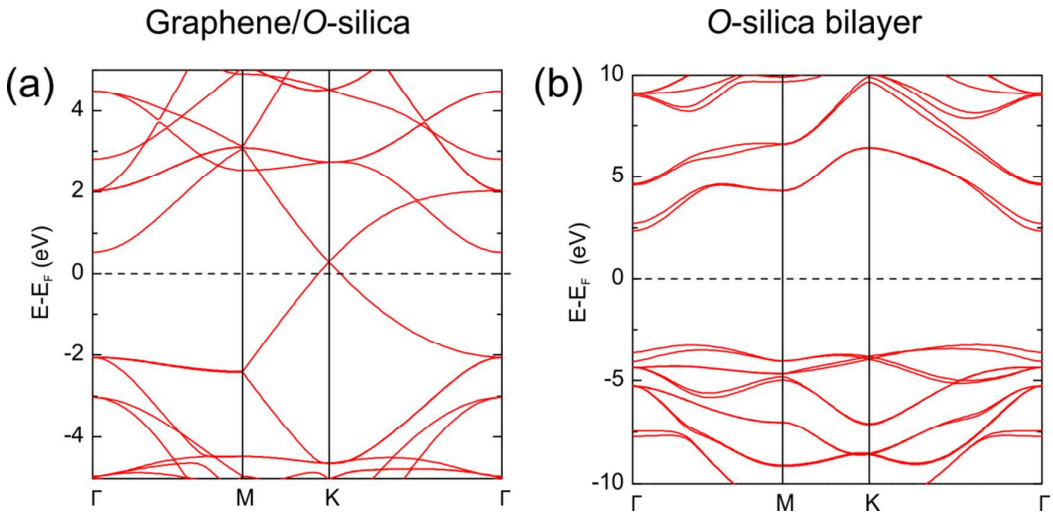

Figure S12 Band structure of (a) $(2 \times 2)\boldsymbol{R}$ *Graphene/*$\left(\sqrt{3} \times \sqrt{3}\right)\boldsymbol{R}$ *O-silica heterostructure, and (b) O-silica bilayer. The Dirac cone of graphene is maintained in the graphene/O-silica bilayer.*

REFERENCES

1. Wang, Y.; Lv, J.; Zhu, L.; Ma, Y., Crystal structure prediction via particle-swarm optimization. *Phys. Rev. B* **2010,** *82*, 094116.
2. Wang, Y.; Lv, J.; Zhu, L.; Ma, Y., CALYPSO: A method for crystal structure prediction. *Comput. Phys. Commun.* **2012,** *183*, 2063-2070.
3. Kresse, G.; Furthmüller, J., Efficiency of ab-initio total energy calculations for metals and semiconductors using a plane-wave basis set. *Comput. Mater. Sci.* **1996,** *6*, 15-50.
4. Kresse, G.; Joubert, D., From ultrasoft pseudopotentials to the projector augmented-wave method. *Phys. Rev. B* **1999,** *59*, 1758-1775.
5. Peng, F.; Miao, M.; Wang, H.; Li, Q.; Ma, Y., Predicted lithium–boron compounds under high pressure. *J. Am. Chem. Soc.* **2012,** *134*, 18599-18605.
6. Luo, X.; Yang, J.; Liu, H.; Wu, X.; Wang, Y.; Ma, Y.; Wei, S.-H.; Gong, X.; Xiang, H., Predicting two-dimensional boron–carbon compounds by the global optimization method. *J. Am. Chem. Soc.* **2011,** *133*, 16285-16290.
7. Perdew, J. P.; Burke, K.; Ernzerhof, M., Generalized Gradient Approximation Made Simple. *Phys. Rev. Lett.* **1996,** *77*, 3865-3868.
8. Bader, R. F., A quantum theory of molecular structure and its applications. *Chem. Rev.* **1991,** *91*, 893-928.
9. Sagar, R. P.; Ku, A. C.; Smith Jr, V. H.; Simas, A. M., The Laplacian of the charge density and its relationship to the shell structure of atoms and ions. *J. Chem. Phys.* **1988,** *88*, 4367-4374.